Interpretation of Quench-Sensitivity in Al-Zn-Mg-Cu Alloys

M. CONSERVA AND P. FIORINI

Electron microscopy and electrical resistivity measurements have been employed to investigate the effect of quenching rates on alloys with a base composition of Al-Zn 5.5 pct-Mg 2.5 pct-Cu 1.6 pct with minor additions of chromium and zirconium, and without other elements. The results show that the loss of aging capability, measured in terms of G.P. zone density, observed after a slow quenching, is to be ascribed to the loss of solute occurring by the formation of large η particles during cooling; therefore, other mechanisms are not required to account for the quench sensitivity of these alloys. In addition, a semi-quantitative relation between high temperature dispersoids and coarse η particles formed during slow quenching has been obtained, bringing new evidence that the different nucleant effect of chromium-rich particles with respect to those containing zirconium is of qualitative character.

IN recent studies[1,2] it was reported that the quench sensitivity* of Al-Zn-Mg-Cu alloy containing chromium is closely connected with the formation of coarse $MgZn_2$-type precipitates that are nucleated, during slow quenching, at the surface of the preexisting chromium-rich E particles. Moreover, it was shown that the addition-free and zirconium-modified alloys do not exhibit any heterogeneous precipitation of $MgZn_2$ particles, or any significant decrease of strength in the investigated quenching rates. On the basis of these results, we have accounted for quench sensitivity in terms of the previously proposed "loss of solute" mechanisms,[3-6] that is by admitting that the formation of large η precipitates, depleting the matrix of solute available for aging, causes a marked decrease of hardening capability of the alloys.

*The term "quench sensitivity" indicates the reduction in age hardening capability induced by low quenching rates.

In contrast with this generally accepted view, some authors have recently proposed a failure mechanism, involving a weak interface between the large η particles, formed during quenching, and the matrix, to account for the loss of strength at low quenching rates.[7]

In order to support the mechanism based on the loss of solute with more convincing experimental evidence we have performed further investigations by electrical resistivity measurements and transmission electron microscopy (TEM) examinations.

The aim of these experiments was twofold:

i) to estimate the decrease of G.P. zone density (taken as an index of the aging capability) induced by a slow quenching;

ii) to relate the density of high temperature dispersoids containing chromium and zirconium to the heterogeneous precipitation of η $MgZn_2$ particles.

1) EXPERIMENTAL

Three high purity alloys of nominal composition (in wt pct) Al-5.5 pct Zn-2.5 pct Mg-1.6 pct Cu were used in the present investigation, with chromium and zirconium, respectively, and without other addition elements, Table I. The experimental samples were 0.18 mm thick sheets, prepared from D.C. ingots, 110 mm in diameter. After homogenizing at 440°C for 24 h transverse slices were cut from the ingots, hot rolled at 430° to 380°C and subsequently cold rolled to the final thickness, with an intermediate annealing at 350°C.

Resistivity experiments were carried out directly on the sheets using 60 by 5 by 0.18 mm specimens and performing the measurements in liquid nitrogen by the standard potentiometric method; the resistivity variations were calculated by the formula:

$$\Delta\rho = \rho_0 \frac{\Delta R}{R_0}$$

ΔR being the resistance variation after any treatment, R_0 and ρ_0 the resistance and resistivity, respectively, of the alloys after fast quenching from 465°C.

Transmission electron microscopy examinations were performed on the same resistivity samples, after electrolytic thinning at −35°C, using a solution of 3 parts of CH_3OH, 1 part of concentrated HNO_3 by volume (potential 15 V, current density 1 amp/cm^2).

In Table I we reported the values of ρ_0 at −196°C for the three alloys after fast quenching at 0°C from 465°C; by comparing the values of ρ_0, on the assumption that the contribution to resistivity α and β of 1 at. pct of chromium and zirconium, respectively, is not influenced by the presence of the other solute atoms, it is possible to estimate the fraction of these ancillary elements which is out of the solid solution. Now from measurements on binary alloys, we have found $\alpha = 8.6\ \mu\Omega$ cm and $\beta = 8.1\ \mu\Omega$ cm. Therefore it is easily computed that the fraction of chromium and zirconium out of the solid solution is about 70 and 80 pct, respectively.

The samples, solution treated at 465°C for 1 h, were quenched in three different ways to get the following cooling rates, constant in the temperature range 465° to 250°C: i) 20,000°C/s (high rate); ii) 15°C/s (slow rate); iii) 4°C/s (very slow rate). The rate of 20,000°C/s has been selected to get the highest response to aging; 15° and 4°C/s can be considered in the critical range of quenching of commercial Al-Zn-Mg-Cu alloys.

After every quenching treatment, the samples were first dipped into brine at 2°C and immediately afterwards into liquid nitrogen for resistivity measurement; the aging treatment was performed at 60°C.

M. CONSERVA and P. FIORINI are Research Metallurgists, Istituto Sperimentale dei Metalli Leggeri, Novara, Italy.

Manuscript submitted April 3, 1972.

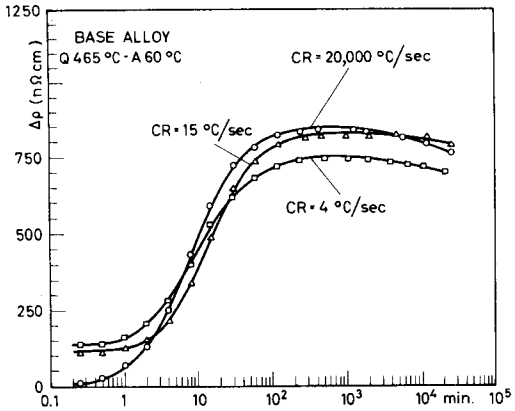

Fig. 1—Isothermal aging curves at 60°C of the base alloy after quenching from 465°C with different cooling rates (CR).

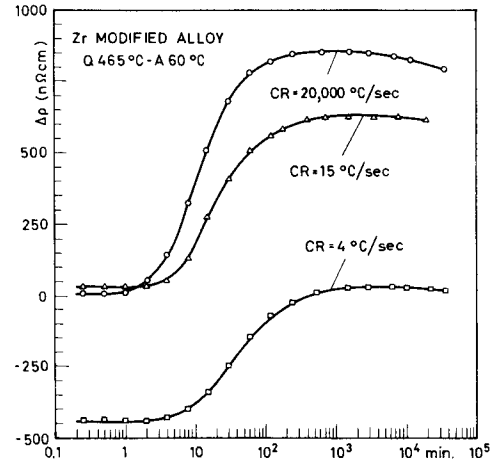

Fig. 2—Isothermal aging curves at 60°C of the zirconium-modified alloy after quenching from 465°C with different cooling rates (CR).

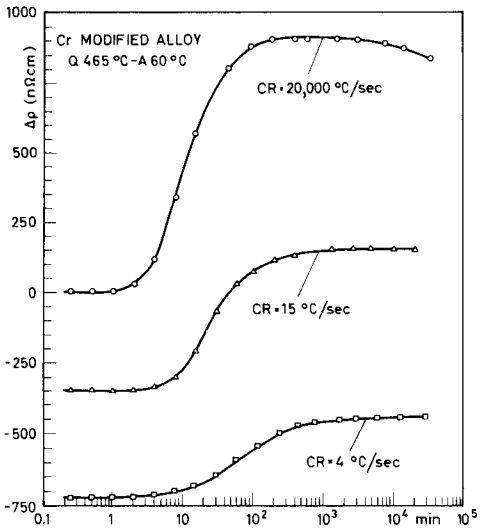

Fig. 3—Isothermal aging curves at 60°C of the chromium-modified alloy after quenching from 465°C with different cooling rates (CR).

2) RESULTS AND DISCUSSION

a) Resistivity Measurements

Figs. 1 to 3 show resistometric aging curves at 60°C after the three different quenching rates for base, zirconium-modified and chromium-modified alloys, respectively. The resistivity value after quenching in each curve is indicated by an horizontal segment.

Before analyzing the results, we summarize the basic assumptions regarding the resistivity variations connected to the clustering process in the aluminum alloys:[8,9]

a) each cluster or G.P. zone provides an independent contribution to the resistivity; b) this contribution can be expressed by a function $\phi(r)$, where r is the dimension of the zone. The function $\phi(r)$ increases with r when r is small, passes through a maximum for a critical value of r (r_c) and then declines when $r > r_c$.

Let us first consider the base alloy: as one can see from the curves of Fig. 1 the dependence of the aging process on the quenching rate is slight. In all cases, as revealed by the resistivity increase, G.P. zone formation takes place during the aging. However, after the slow and the very slow quenching rate a resistivity increase is already present after quenching, indicating that some clustering of solute atoms has occurred during the very quenching. In addition, the slightly lower values of resistivity maximum reached during the aging can suggest that some loss of solute takes place during quenching. The presence of zirconium and chromium, Figs. 2 and 3, does not influence the aging process after fast quenching, whereas it plays a significant role after slow and very slow quenching. In detail, zirconium-modified alloy shows a resistivity increase after slow quenching that is due to a clustering process, which appears lower than the one observed in base alloy; therefore, one can infer that a partial loss of solute occurs during quenching, in agreement with the lower resistivity maximum observed during aging. After very slow quenching the alloy reaches a high negative resistivity value due to solute precipitation and the aging process is very reduced with respect to fast quenching.

The resistivity values of the chromium-modified alloy, Fig. 3, after slow and very slow quenching are strongly negative, showing that precipitation of solute is very pronounced; in this case too, the higher is the loss of solute during quenching, the lower is the resistivity increase during aging.

Assuming that the precipitation produced during the quenching is qualitatively characterized by the formation of the same type of phase, it is possible to obtain an estimation of the relative loss of solute in the different alloys from the resistivity values after quenching and from the resistivity maximum.

This loss of solute is always negligible after fast quenching and small after slow and very slow quenching in the base alloy. It becomes appreciable for slowly quenched zirconium-modified alloy and it is very remarkable in all other cases. In particular it can be pointed out that the precipitate fraction is nearly the same for very slowly quenched zirconium-modified alloy and slowly quenched chromium-modified alloy, whereas it is nearly double for very slowly quenched chromium-modified alloy.

An important result arising from the analysis of the data is the fact that all the curves of Figs. 1, 2, and 3 have the same analytical shape. Indeed, they can be superimposed when plotted in a normalized form, as shown in Fig. 4. Superimposition is obtained by prop-

Table I. Chemical Composition of the Investigated Alloys and Resistivity Values at −196°C After Fast Quenching to 0°C

Alloy Type	Zn Pct	Mg Pct	Cu Pct	Fe Pct	Si Pct	Ti Pct	Cr Pct	Zr Pct	ρ_0, nΩ cm at 196°C
base	5.64	2.46	1.61	0.0010	0.0026	0.015			2525
Zr modified	5.58	2.45	1.57	0.0041	0.0012	0.019		0.22	2632
Cr modified	5.56	2.44	1.59	0.0015	0.0020	0.015	0.23		2857

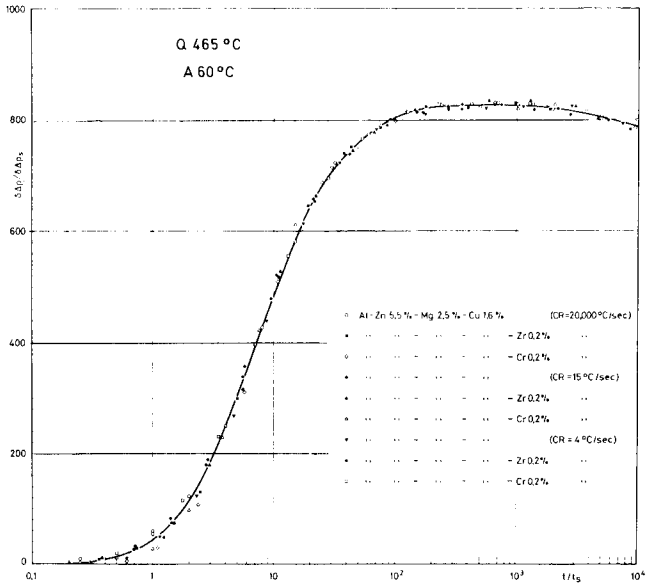

Fig. 4—Superimposition of the experimental curves of Figs. 1 to 3 normalized with respect to the aging times and resistivity increase.

erly changing the time and the resistivity scale, namely by reporting $\delta\Delta\rho/\delta\Delta\rho_S$ vs t/t_S, $\delta\Delta\rho$ being the resistivity variations computed from the resistivity values after the relative quenching. The normalizing t_S and $\delta\Delta\rho_S$ values are given in Table II. t_S is a parameter which accounts for the difference in the diffusion rate mainly due to the difference in the vacancy concentration; $\delta\Delta\rho_S$ is a parameter which accounts for the difference in G.P. zone density resulting from the different supersaturation. As discussed in previous papers,[8-10] the result of Fig. 4 indicates that the nature of the aging process is always the same. The density of G.P. zones changes from one curve to another (varying the supersaturation of the alloys as a consequence of the loss of solute during quenching) and also the kinetics of the process changes (varying the vacancy concentration), but the kind of zones and the law zone growth remain unchanged. From the ratio between $\delta\Delta\rho_S$ values we can obtain an estimate of the ratio between the G.P. zone density in the investigated alloys for different quenching procedure: thus, for example, it is possible to see that in chromium-modified alloy the G.P. zone density, after very slow quenching is more than three times lower than after fast quenching. Moreover the values of t_S directly give a relative index of the kinetics in the different cases.

The results of Fig. 4 also confirm the validity of the hypothesis previously assumed to evaluate the relative precipitate fraction during slow quenching.

Table II. Parameters Characterizing the Resistivity Curves

Alloy Type	Cooling Rate 20,000°C/s $\delta\Delta\rho_s$, nΩ cm	20,000°C/s t_s, min	15°C/s $\delta\Delta\rho_s$, nΩ cm	15°C/s t_s, min	4°C/s $\delta\Delta\rho_s$, nΩ cm	4°C/s t_s, min
base	1.00	1.0	0.83	1.7	0.77	1.4
Zr modified	1.02	1.6	0.71	2.7	0.57	5.5
Cr modified	1.09	1.7	0.62	4.6	0.31	8.5

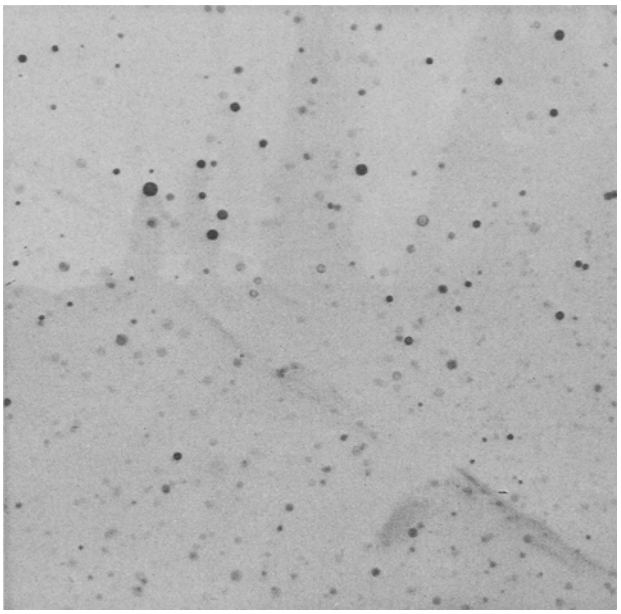

Fig. 5—Distribution of $ZrAl_3$ particles in zirconium-modified alloy after fast quenching. The precipitates exhibit different contrast effects as a consequence of their orientation. Magnification 60,000 times.

b) Microstructures

TEM observations were performed with the main purpose of obtaining quantitative data about the various precipitated phases present in the alloys after different quenching experiments.

The microstructural results have been analyzed according to the expression

$$N_a = N_v(t + \bar{K})$$

where

N_a = number of particles for $(\mu m)^2$, measured on 5 micrographs (standard magnification of X40,000) for each state)

N_v = number of particles for cm^3

t = thickness of the thin foil, considered constant and ≃2000Å

$\bar{K}$ = mean diameter of the particles in Å, measured with the same procedures as N_a

The following results have been obtained:

i) Fast quenching (20,000°C/s)—η particles, intergranular or intragranular have been detected in none of the three alloys.

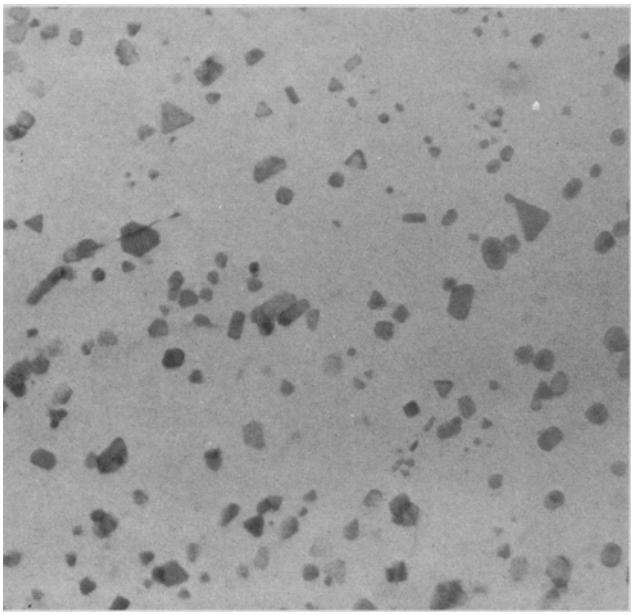

Fig. 6—Distribution of E dispersoids in chromium-modified alloy after fast quenching. Magnification 60,000 times.

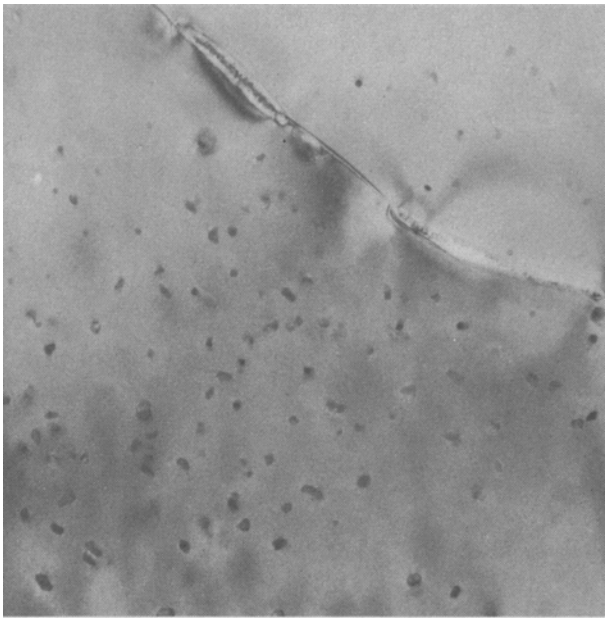

Fig. 7—Microstructure of the zirconium-modified alloy after slow quenching. Magnification 60,000 times.

Zirconium-modified alloy exhibits a fine distribution of $ZrAl_3$ semicoherent compounds, with $\bar{K} \simeq 180$Å and $N_v \simeq 8 \cdot 10^{14}/cm^3$, Fig. 5; chromium-modified alloy is characterized by the precipitation of E dispersoids with $\bar{K} \simeq 400$Å and $N_v \simeq 4 \cdot 10^{14}/cm^3$, Fig. 6.

ii) Slow quenching (15°C/s)—In some grain boundaries of the base alloy, few and coarse particles of $MgZn_2$ are visible.

In the zirconium-modified alloy small η particles (200 to 300Å diam) of irregular shape and distribution, all nucleated at $ZrAl_3$ compounds, may be observed; furthermore, some intergranular η particles are present, Fig. 7.

A direct relation between the high temperature dispersoids and the η particles is seen in chromium-modified alloy; in Fig. 8 it is evident that $MgZn_2$ precipitates have a definite platelet shape, with an average size of about 1000Å.

In most cases, colonies of η particles nucleated by single E dispersoids have been observed.

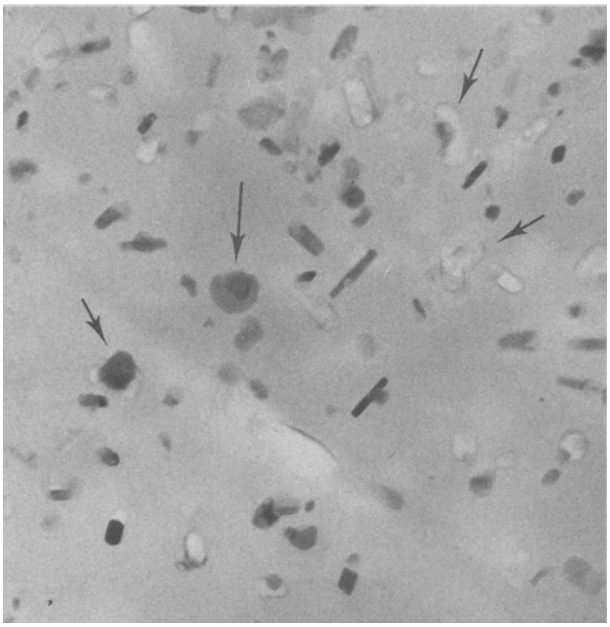

Fig. 8—Microstructure of the chromium-modified alloy after slow quenching. The arrows show coarse η precipitates in association with E particles. Magnification 60,000 times.

iii) Very slow quenching (4°C/s)–Some precipitation phenomena are seen in the base alloy.

Zirconium-modified alloy exhibits, in this state, dense general precipitation of η particles uniformly dispersed in the matrix and along grain and subgrain boundaries, Fig. 9(a); high magnification micrograph, Fig. 9(b), shows that η particles, with an average diameter of ~700 to 800Å, are in close association with the spherical $ZrAl_3$ precipitates.

Finally, the very slow quenching of chromium-containing alloy produces a precipitation of $MgZn_2$ particles, with an average size of ~2500Å, much denser than the E dispersoids, Figs. 10(a) and 10(b).

All the data relative to the structural parameters of the studied alloys are summarized in Table III. It can be observed that the density of η particles formed during the quenching of zirconium-modified alloy, is less than, or the same as, $ZrAl_3$ particles, while it is even higher than the E phase in chromium-modified alloy. In addition, with identical cooling conditions, chromium-containing alloy is characterized by coarser $MgZn_2$ particles. These data, considering that the density of $ZrAl_3$ dispersoids is higher than E particles, mean that the different behavior of zirconium-modified alloy with respect to the chromium-containing one is really qualitative. In fact, it does not depend on the different density of high temperature precipitation, but rather, it seems to be linked to the different nucleant action of the E phase with respect to $ZrAl_3$ particles. This experimental evidence completely agrees with our previ-

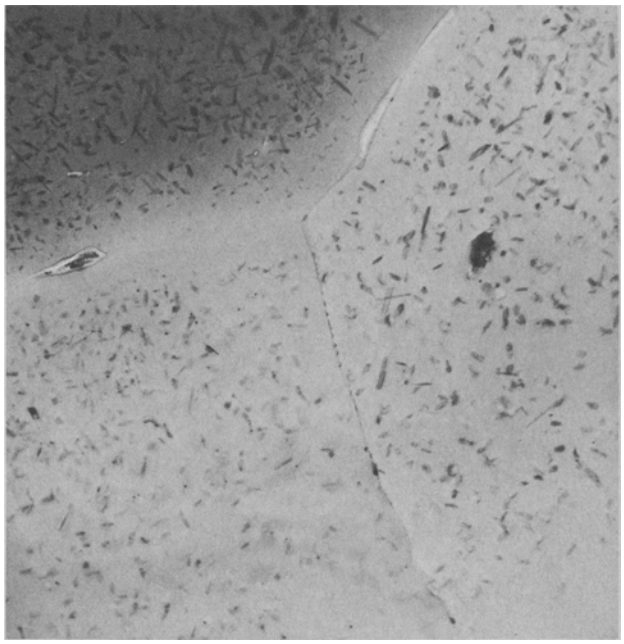

(a)

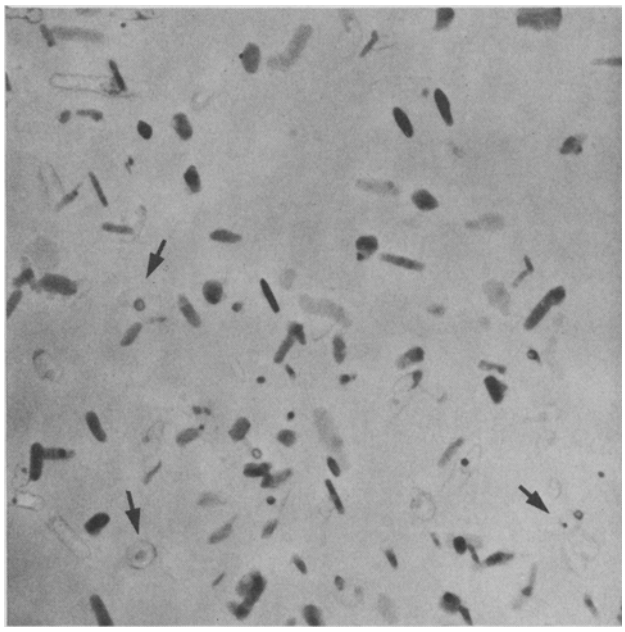

(b)

Fig. 9—Microstructure of the zirconium-modified alloy after very slow quenching: (*a*) magnification 20,000 times; (*b*) magnification 60,000 times. The arrows show coarse η precipitates in association with $ZrAl_3$ particles.

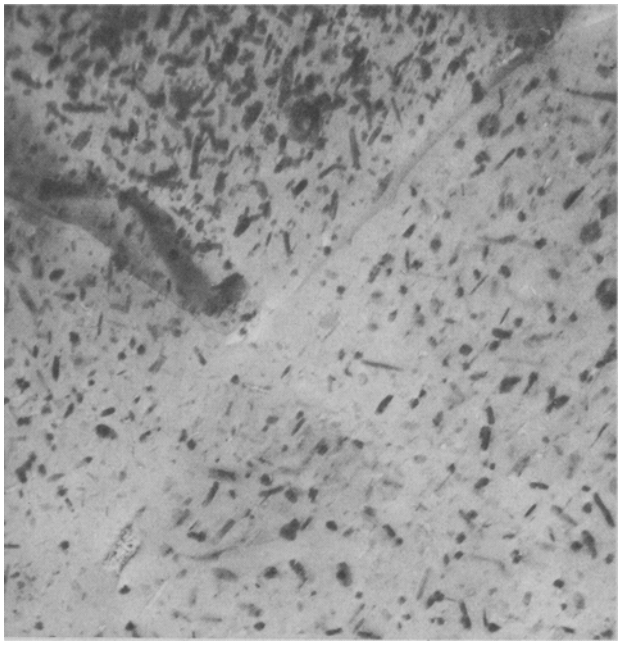

(a)

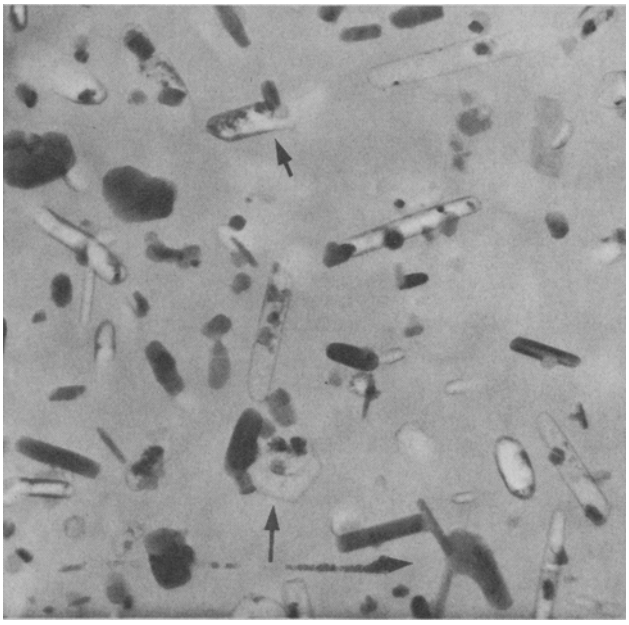

(b)

Fig. 10—Microstructure of the chromium-modified alloy after very slow quenching: (*a*) magnification 20,000 times; (*b*) magnification 60,000 times. The arrows show colonies of η precipitates nucleated at E particles.

ous findings[1] and, considering the different crystallographic features of the two types of precipitates, with theory.[11]

3) CONCLUSIONS

By resistivity measurements and TEM observations a detailed analysis has been performed of:

a) the quench induced precipitation of high purity Al-Zn-Mg-Cu alloy with chromium and zirconium and without other addition elements;

b) the influence exerted by the loss of solute occurring during the quenching on the G.P. zone formation.

The starting structures of the chromium and zirconium containing alloys were characterized respectively by a high temperature precipitation of $\sim 4 \cdot 10^{14}$ particles/cm^3 of E phase and $\sim 8 \cdot 10^{14}$ particles/cm^3 of $ZrAl_3$ phase.

The cooling rates investigated were the following: 20,000°C/s, 15°C/s, 4°C/s, in the interval 465° to 250°C.

In these experimental conditions, the obtained results may be summarized as follows:

Table III. Relation Between the Cooling Rate and Microstructural Properties of the Investigated Alloys

Cooling Rate	Structural Parameters	Base Alloy	Zr Modified Alloy	Cr Modified Alloy
20,000°C/s	grain structure (g.s.)	equiaxic grains	grains and subgrains	
	matrix (m.)	homogeneous solid solution	solid solution with dispersoids of: $ZrAl_3$: $\bar{K} \simeq 180$Å, $N_v \simeq 8.10^{14}$	$Al_{18}Cr_2Mg_3$: $\bar{K} \simeq 400$Å, $N_v \simeq 4.10^{14}$
	intragranular precipitation (i.p.)		absent	
	grain boundaries precipitation (b.p.)		almost absent	
15°C/s	g.s.	the same as 20,000°C/s	the same as 20,000°C/s	
	m.	the same as 20,000°C/s	the same as 20,000°C/s	
	i.p.	the same as 20,000°C/s	η particles: very fine and rare $\bar{K} \simeq 250$Å, $N_v \simeq 8.10^{14}$	η particles: rather dense and coarse $\bar{K} \simeq 1000$Å, $N_v \simeq 4.10^{14}$
	b.p.		the same cases as coarse η precipitation	
4°C/s	g.s.	the same as 20,000°C/s	the same as 20,000°C/s	
	m.	the same as 20,000°C/s	the same as 20,000°C/s	
	i.p.	the same as 20,000°C/s	η particles: rather dense $\bar{K} \simeq 500$Å, $N_v \simeq 8.10^{14}$	η particles: very dense and coarse $\bar{K} \simeq 2500$Å, $N_v \simeq 1.10^{15}$
	b.p.		frequent precipitation of coarse η particles	

i) the presence of chromium and zirconium does not produce a significant effect on the G.P. zone aging process after fast quenching;

ii) the base alloy does not exhibit any noticeable precipitation, also for the very slow quenching rate;

iii) a close association exists between the compounds of the addition elements and the quench induced precipitation of $MgZn_2$. For the same quenching conditions, η particles are denser and coarser in chromium containing alloy, probably due to the different nucleant action exerted by E dispersoids with respect to $ZrAl_3$ globules. Moreover, it is to be stressed that in zirconium-modified alloy the slow quenching treatment (15°C/s) produces a slight precipitation of η phase, so that this cooling rate may be practically considered the upper level of the quench sensitivity of this alloy;

iv) the aging response of the alloys strongly depends on the precipitation induced by quenching. However, the aging mechanisms remain unchanged, the cooling rate differences only determining a variation of the supersaturation of the alloys and of the vacancy concentration. This circumstance has permitted a correlation between the solute fraction precipitated during the quenching and the consequent decrease in aging capability, measured in terms of G.P. zone density. Hence, other factors are not required to account for the quench-sensitivity phenomenon.

ACKNOWLEDGMENTS

This work was partially sponsored by the Italian Ministry of Defence and the U.S. Department of the Army, according to U.S./Italy Cooperative Research and Development Project on Aluminum Alloys.

REFERENCES

1. M. Conserva, E. Di Russo, and O. Caloni: *Met. Trans.*, 1971, vol. 2, pp. 1227-32.
2. M. Conserva and E. Di Russo: *I.S.M.L. Quaderno Mono.*, 1972, no. 15.
3. W. L. Fink and L. A. Willey: *Tech. Publ.*, no. 2225, *Metals Tech.*, 1947, vol. 14.
4. E. Di Russo: *I.S.M.L. Internal Report*, 1965, no. 14601.
5. A. J. Bryant: *J. Inst. Metals*, 1966, vol. 94, pp. 94-99.
6. H. A. Holl: *J. Inst. Metals*, 1969, vol. 97, pp. 200-05.
7. D. S. Thompson, B. S. Subramanya, and S. A. Levy: *Met. Trans.*, 1971, vol. 2, pp. 1149-60.
8. C. Panseri and T. Federighi: *Acta Met.*, 1960, vol. 8, pp. 217-38.
9. C. Panseri and T. Federighi: *J. Inst. Metals*, 1966, vol. 94, pp. 99-107.
10. S. Ceresara, E. Di Russo, P. Fiorini, and A. Giarda: *Mater. Sci. Eng.*, 1969-70, vol. 5, pp. 220-27.
11. R. B. Nicholson: in *Phase Transformation*, p. 300, ASM, 1970.